APPENDIX B
A REFERENCE ON HOW TO INCORPORATE CREDIBLE HUMAN ENZYME STUDIES INTO THE PHYSIOLOGICALLY-BASED PHARMACOKINETIC (PBPK) MODELING AND RISK ASSESSMENT PROCESS

Lipscomb, J.C., L.K. Teuschler, J. Swartout, D. Popken, T. Cox and G.L. Kedderis. 2003. The impact of cytochrome P450 2E1-dependent metabolic variance on a risk-relevant pharmacokinetic outcome in humans. Risk. Anal. 23(6):1221-1238.

Risk Analysis, Vol. 23, No. 6, 2003

The Impact of Cytochrome P450 2E1-Dependent Metabolic Variance on a Risk-Relevant Pharmacokinetic Outcome in Humans

John C. Lipscomb,[1]* Linda K. Teuschler,[1] Jeff Swartout,[1] Doug Popken,[2] Tony Cox,[2] and Gregory L. Kedderis[3]

Risk assessments include assumptions about sensitive subpopulations, such as the fraction of the general population that is sensitive and the extent that biochemical or physiological attributes influence sensitivity. Uncertainty factors (UF) account for both pharmacokinetic (PK) and pharmacodynamic (PD) components, allowing the inclusion of risk-relevant information to replace default assumptions about PK and PD variance (uncertainty). Large numbers of human organ donor samples and recent advances in methods to extrapolate *in vitro* enzyme expression and activity data to the intact human enable the investigation of the impact of PK variability on human susceptibility. The hepatotoxicity of trichloroethylene (TCE) is mediated by acid metabolites formed by cytochrome P450 2E1 (CYP2E1) oxidation, and differences in the CYP2E1 expression are hypothesized to affect susceptibility to TCE's liver injury. This study was designed specifically to examine the contribution of statistically quantified variance in enzyme content and activity on the risk of hepatotoxic injury among adult humans. We combined data sets describing (1) the microsomal protein content of human liver, (2) the CYP2E1 content of human liver microsomal protein, and (3) the *in vitro* V_{max} for TCE oxidation by humans. The 5th and 95th percentiles of the resulting distribution (TCE oxidized per minute per gram liver) differed by approximately sixfold. These values were converted to mg TCE oxidized/h/kg body mass and incorporated in a human PBPK model. Simulations of 8-hour inhalation exposure to 50 ppm and oral exposure to 5 g TCE/L in 2 L drinking water showed that the amount of TCE oxidized in the liver differs by 2% or less under extreme values of CYP2E1 expression and activity (here, selected as the 5th and 95th percentiles of the resulting distribution). This indicates that differences in enzyme expression and TCE oxidation among the central 90% of the adult human population account for approximately 2% of the difference in production of the risk-relevant PK outcome for TCE-mediated liver injury. Integration of *in vitro* metabolism information into physiological models may reduce the uncertainties associated with risk contributions of differences in enzyme expression and the UF that represent PK variability.

KEY WORDS: Cytochrome P450 2E1 (CYP2E1); interindividual differences; physiologically-based pharmacokinetic modeling; risk assessment; trichloroethylene bioactivation; uncertainty factors

[1] U.S. EPA, ORD, NCEA, Cincinnati, OH, USA.
[2] Cox Associates, Denver, CO, USA.
[3] Independent Consultant, Chapel Hill, NC, USA.
* Address correspondence to John C. Lipscomb, PhD, DABT, U.S. EPA/ORD/NCEA, 26 W. M.L. King Drive, MD-190, Cincinnati, OH 45268, USA; Lipscomb.John@EPA.GOV

1. INTRODUCTION

Traditional noncancer risk assessments in the U.S. EPA apply uncertainty factors to extrapolate the measures of effects between animals and humans,

0272-4332/03/1200-1221$22.00/1

and among humans. These two factors (UFA and UFH, respectively), may be further subdivided into their respective pharmacodynamic (PD) and pharmacokinetic (PK) components.[1–3] WHO[4] and the International Programme on Chemical Safety[5,6] have provided guidance and application of the separate consideration of PD and PK, and the U.S. EPA has also separately quantified PD and PK variability in the UFA applied to reference concentration (RfC) values and reference dose (RfD) values, where each has been ascribed a default value of one-half log ($10^{0.5}$, or 3.16).[7–9] In addition, PD and PK components of UFH for RfC values have also been separately considered for some substances such as methyl methacrylate.[10] Studies with humans can be conducted to assess the pharmacodynamics or pharmacokinetics of environmental or occupational chemicals. While human clinical trials can assess the PK and PD of potential therapeutic substances, human studies with potentially toxic environmental or occupational chemicals are not usually conducted over concentration ranges known or predicted to result in adverse effects. The limited information available from human studies with environmental chemicals provides critical (but often limited) information, which can be extended by *in vitro* studies using preparations from human tissues. Care must be taken so that the *in vitro* investigations are focused on risk-relevant endpoints, and are conducted with the relevant tissues, tissue preparations, and chemical concentrations. It is critical that the concentrations used for *in vitro* studies are within the range of tissue concentrations observed or predicted *in vivo* in humans following chemical exposure. Studies with human subjects or human tissue preparations *in vitro* can identify variability in PK outcomes such as the blood concentrations of parent chemical and metabolites or the rates of metabolite production or elimination. When these PK outcomes overlap with the PK outcomes most linked to risk (verified by results from mode of action and PK studies with research animals), then additional information on the variability of these PK outcomes will advance our understanding of susceptibility, and provide information with which to replace default values for uncertainty in extrapolations of risk. Although data from multiple human subjects may seem preferable as the basis from which to determine human PK variability, those data seldom exist, and when they do the data usually offer little information on risk-relevant PK outcomes such as target tissue dosimetry. Physiologically-based PK (PBPK) models allow the application of physiologic

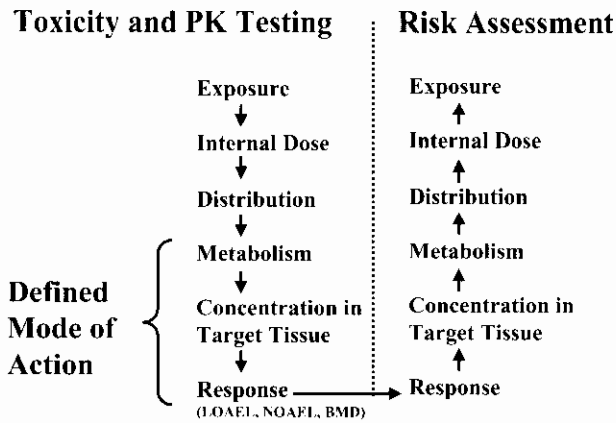

Fig. 1. Application of PBPK modeling to link external dose with concentration of toxicant in target organs. The approach builds upon information on mode of action, which demonstrates the relationship between tissue response, a PD phenomenon, and the PK outcome directly related to that response. PBPK models are then developed and employed to define the relationship between the external exposure and the target organ toxicant concentration, usually performed in test animal species. Once completed, and based on assumptions about the similarity in the qualitative and quantitative nature of the PD effect (mode of action) between the test species and humans, parallel PBPK models are developed for the human, and are exercised to "back-track" the toxicant from a predetermined concentration in the target tissue to the corresponding exposure concentration (external dose).

and anatomic constraints to clarify the linkage between external concentrations and target tissue concentrations (Fig. 1) and offer a mechanism through which information obtained *ex vivo* or *in vitro* may be evaluated in the proper context. Results from PBPK model simulations of relevant exposure scenarios provide a useful approach for estimation of PK variability between research animals and humans and among humans when other data are limiting. This technique offers the opportunity to extrapolate concentrations of bioactive chemical moieties in target tissues across species, doses, and routes of exposure. The inclusion of data derived *in vitro* through the exposure of human tissue preparations offers an advance over exposing humans to noxious agents, and several studies have demonstrated the applicability of *in vitro* findings in refining PBPK models.

While *in vitro* measurements of specific biochemical reactions from multiple human samples can yield qualitatively valuable data on human variance, they must be tied to human anatomy and physiology, and the impact of their variance evaluated under real exposure scenarios, to be of quantitative value. This

study was constructed on the framework for extrapolation of *in vitro* metabolic rate information and PBPK model incorporation previously suggested.[11]

Enzymes are protein molecules that catalyze chemical reactions.[12] Over 100 years ago, the study of enzymes and their properties demonstrated that the rates of enzyme-catalyzed reactions are directly proportional to the total enzyme present in the system.[12,13] This property of enzymes provides the basis for extrapolation of *in vitro* biotransformation data to whole animals and humans.[14] Therefore, data generated with subcellular fractions such as microsomes or cytosols can be extrapolated to *in vivo* based on protein content.[15] Human liver is approximately 2.6% of body weight.[16]

In addition to enzyme content or activity and organ weight, the kinetic mechanism of the enzyme (the comings and goings of substrates and products) needs to be taken into account to extrapolate *in vitro* data to whole animals or humans.[14] The CYP2E1-catalyzed oxidation of TCE follows Michaelis-Menten saturation kinetics:[17]

$$v = (V\max * [S])/(K_M + [S]) \qquad (1)$$

where v is the initial velocity of the reaction, V_{max} is the maximal rate of the reaction at infinite substrate concentration, $[S]$ is the substrate concentration, and K_M is the Michaelis constant for the reaction. The Michaelis-Menten (Equation (1)) indicates that the initial velocity of the reaction will increase hyperbolically as a function of substrate concentration. The V_{max} is a horizontal tangent to the top (saturated) part of the curve, while the tangent to the initial linear portion of the hyperbolic curve is the initial rate of the reaction, V/K. The V/K is the pseudo-first-order rate constant for the reaction at low substrate concentrations. The point where these two tangents intersect corresponds to the K_M.[18] The K_M is defined as the substrate concentration that gives one-half the V_{max}. The K_M for each substrate is an inherent property of the enzyme.[12] A lower K_M for one substrate compared to a second substrate indicates that the first substrate has a more rapid initial rate (V/K) of metabolism. The value of K_M can vary with the structure of the enzyme; for example, in the polymorphism of the CYP2D6-mediated oxidation of debrisoquine and related drugs.[19] Experimentally, K_M can vary with pH, temperature, and ionic strength *in vitro*. Therefore, *in vitro* kinetic measurements intended for extrapolation to intact animals and humans should be done under experimental conditions mirroring the *in vivo* situation as closely as possible.[14]

The *in vitro* kinetic data can be incorporated into PBPK models after rearrangement of the V_{max} to the appropriate units. Values of K_M have units of concentration and can be used directly if the solubility of the chemical in the *in vitro* system is known. Incorporation of the extrapolated kinetic parameters into a PBPK model for humans allows prediction of target tissue dosimetry following a variety of exposure scenarios.

We have adapted an existing PBPK model to predict the difference among humans in the risk-relevant PK outcome for the hepatotoxicity of trichloroethylene (TCE) under conditions of human variance in the rates of TCE oxidation. We focused on the hepatotoxicity of TCE because: (1) the PK of TCE have been characterized and modeled in research animals and humans (reviewed in Reference (20); (2) more than 95% of an absorbed dose of TCE is oxidized in research animals and humans;[21] (3) CYP2E1 has been demonstrated to be the enzyme responsible for the oxidation of TCE in research animals and humans and *in vitro* preparations at low concentrations;[22] (4) the hepatotoxicity of TCE has been demonstrated to depend on acid metabolite(s) derived from oxidative metabolites of TCE;[23,24] (5) the CYP2E1-mediated oxidation of TCE is rate limiting in the further formation of acid metabolite(s);[25] (6) the expression of CYP2E1 is modulated by genetic, environmental, and lifestyle factors; and (7) large numbers of human liver tissue samples and human liver tissue preparations are currently available in contrast with preparations and tissues from other human organs. The results on the variance of the distribution of CYP2E1 in adult human liver will be especially applicable to other environmental contaminants that are also substrates for this enzyme.

The investigation was accomplished by first characterizing the variance about the CYP2E1-mediated oxidation of TCE among human samples *in vitro*, second by quantifying the variance of human hepatic CYP2E1 content, and third by extrapolating the bounds of variance of TCE oxidation among the adult human population to a human PBPK model. Two separate statistical analyses were conducted—one based on convenience and one based on technical accuracy. The amount of TCE metabolized (oxidized) in the liver was simulated as a dose surrogate for the hepatotoxicity of TCE. The goal of the present investigation was to quantify the variability in a risk-relevant PK outcome for the hepatotoxicity of TCE, and to demonstrate the usefulness of advanced data on human biochemical individuality in quantifying the

variability of risk-relevant PK outcomes for inclusion in risk assessments. Data on the distribution of CYP2E1 in the intact liver has not been used to estimate the degree of susceptibility to risk for metabolized chemicals. We hypothesized that the degree of natural variance in human hepatic levels of CYP2E1 would result in similar differences in the oxidation of TCE in the intact human.

2. METHODS

Several sets of information describing or based on microsomal protein (MSP) were collected for assimilation, extrapolation, and incorporation into a PBPK model. The objective of the extrapolation was to transition expression of apparent V_{max} from units of "pmoles TCE oxidized/min/mg MSP" to units of conventional PBPK modeling, mg/h/kg body mass. Necessary data were compiled from multiple sources, and used to describe the various parameters, whose distributions were analyzed and combined. Table I demonstrates the relationship between those data sets and parameters. TCE is oxidized by CYP2E1, and that metabolic rate had been previously measured and presented in units of MSP (nmol/min/mg MSP). Thus, the need to express apparent V_{max} as pmol TCE oxidized/min/pmol CYP2E1. CYP2E1 is isolated in MSP, thus the need to quantify CYP2E1 in MSP (pmoles CYP2E1/mg MSP). Because MSP is one constituent of liver, the amount of MSP per gram liver tissue (mg MSP/gram liver) needed computing. These data facilitate the extrapolation of *in vitro* metabolic capacity (comprising enzyme activity and enzyme content) to the intact liver. Units of calculation cancel (pmol TCE oxidized/min/pmol CYP2E1) × (pmol CYP2E1/mg MSP) × (mg MSP/gram liver), leaving units of pmol TCE oxidized/min/gram liver. Correction for molecular weight of TCE, 60 min/h, and assumptions about the fractional composition of body mass attributed to the liver compartment (liver = BW × 0.026) results in units of mg TCE oxidized/h/kg.

2.1. Human Samples and Quantification of CYP Proteins

Both prepared MSP and intact liver tissue were obtained for this investigation from various sources (Human Cell Culture Center, Laurel, MD; International Institute for the Advancement of Medicine, Exton, PA; Vitron, Tucson, AZ; Tissue Transformation Technologies, Inc., Edison, NJ). All tissues and preparations were derived from adult human organ donors that were devoid of antibodies directed against infectious diseases. The MSP content of CYP2E1 and other CYP forms was previously investigated and reported for 40 donors.[15] In the present analysis, 20 samples of intact tissue were obtained, and MSP prepared via the method of Guengerich[26] (Fig. 2). CYP2E1 content of aliquots of (post 100 × *g*) homogenate protein and MSP were determined by enzyme-linked immunosorbent assay (ELISA) following the method of Snawder and Lipscomb.[15]

2.2. Distribution of CYP2E1 to Human Hepatic MSP

Data on the CYP2E1 content from 40 samples of human hepatic MSP were available from Snawder and Lipscomb,[15] and data derived from an additional 20 samples of human hepatic MSP were

Table I. Identification of Data Sets and Parameters for Statistical Evaluation

Information	Data Set	Units	Parameter	Notes
CYP2E1 content of intact liver		pmol CYP2E1/gram liver	A	Directly measured via ELISA ($n = 20$); and separately predicted statistically
CYP2E1 content of MSP	Data Set 1 ($n = 60$)	pmol CYP2E1/mg MSP	B	Directly measured via ELISA
MSP content of intact liver	Data Set 2 ($n = 20$)	mg MSP/gram liver	C	Derived: C = A/B
TCE metabolized per unit CYP2E1	Data Set 3 ($n = 15$)	pmol TCE/min/ pmol CYP2E1	D	Original measurements from Reference 11 corrected by CYP2E1 content from Reference 18
TCE metabolized per unit of intact liver		pmol TCE oxidized/minute/gram liver	E	Statistically estimated: E = B × C × D; extrapolated to V_{max}

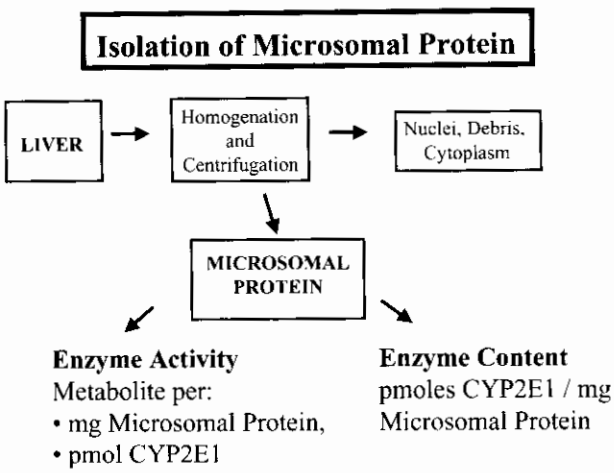

Fig. 2. Relationship between intact liver, microsomal protein, and some CYP forms. The isolation of microsomal protein from intact liver via homogenation of tissue and differential centrifugation results in a 100,000 × *g* pellet, which is enriched for endoplasmic reticulum content. The enrichment results in an artificial increase in the concentration of biological components associated with the endoplasmic reticulum. This isolation produces a fraction (microsomes; MSP), which is subjected to *in vitro* investigations of metabolic activity and enzyme content. However, a quantitative relationship to the intact liver is not possible without further information on the distribution of microsomal protein to the intact liver.

combined to yield a total sample of 60 adult human organ donors for which data on the CYP2E1 content of MSP ($CYP2_{MSP}$, parameter B, data set 1) were available[27] (Table II, described in the following section). Of this set of 60 samples of MSP (representing 60 organ donors), 15 were used to estimate the *in vitro* metabolic parameters for TCE and CYP2E1 content of MSP; 45 were subjected only to the determination of CYP2E1 in MSP (and 20 of that 45 were paired with liver homogenate to determine the MSP content of liver).

2.3. Estimation of Proteins in Intact Liver

In this analysis, 20 samples of intact liver tissue were assayed (Table II). The total amount of protein (CYP and non-CYP; microsomal and cytosolic proteins) in intact liver (PRO_{Liv}) was empirically determined based on the protein content of the post 100 × *g* liver supernatant, after correcting for volume according to Equation (2). It was assumed that no protein was lost during the sedimentation of nuclei and debris at 100 × *g*.

$$\begin{aligned}&(\text{mg protein/ml homogenate})\\&\quad\times(\text{ml homogenate/gram tissue})\\&\quad=(\text{mg homogenate protein/gram tissue})\end{aligned}\qquad(2)$$

The content of CYP2E1 in total hepatic protein ($CYP2_{Pro}$) and in MSP ($CYP2_{MSP}$; parameter B) was determined so that a measure of the liver content of MSP (MSP_{Liv}; parameter C) could be derived. The content of CYP2E1 in liver (pmoles CYP2E1/gram liver; $CYP2_{Liv}$; parameter A) was derived empirically by combining two data sets (PRO_{Liv} CYP_{PRO}), described in Equation (3), and was estimated via the statistical method of moments (Section 2.5.1) and by computational statistics (Section 2.5.2). For the 20 individual organ donors, the separate amounts of CYP2E1 per gram liver were empirically determined according to the following equation:

$$\begin{aligned}&(\text{pmol CYP2E1/mg homogenate protein})\\&\quad\times(\text{mg homogenate protein/gram tissue})\\&\quad=(\text{pmol CYP2E1/gram tissue}).\end{aligned}\qquad(3)$$

The amount of MSP per gram liver was estimated according to Equation (4). This is the data set (MSP_{Liv}; parameter C, data set 2) that will be combined with information on the distribution of CYP2E1 to MSP ($CYP2_{MSP}$; parameter B, data set 1) to determine the distribution of CYP2E1 to the intact liver (CYP_{Liv}; parameter A).

$$\begin{aligned}&(\text{pmol CYP2E1/gram tissue})/\\&\quad(\text{pmol CYP2E1/mg MSP})\\&\quad=(\text{mg MSP/gram tissue})\end{aligned}\qquad(4)$$

2.4. CYP2E1-Dependent Oxidation of TCE

The Michaelis-Menten kinetic constants were available for 23 samples of MSP from Lipscomb *et al.*[17] The metabolism of TCE to chloral hydrate, representing oxidation by CYP2E1, was quantified by measuring the formation of chloral hydrate. Apparent V_{max} was expressed as pmol TCE oxidized/min/mg MSP. From this set of 23 original samples, 15 remained, and CYP2E1 content of those microsomal protein samples was quantified by ELISA.[15] We sought to develop a more technical description of V_{max} (the theoretical maximal initial rate of the reaction in the presence of unlimiting substrate concentration), and one that would be more readily extrapolable to the *in vivo* setting through incorporation of the information on the hepatic content of CYP2E1. To accomplish this, the V_{max} values (pmoles/min/mg MSP) available from the previously published study[17] were divided by the CYP2E1 content of MSP (pmoles CYP2E1/mg MSP)

Table II. Liver Enzyme Data[27]

Samples	Homog. Protein (mg/Gram Liver)	CYP2E1 per mg Homog. Protein	Parameter A = pmol CYP2E1 per Gram Liver	Parameter B = pmol CYP2E1 per mg MSP	Parameter C = mg MSP per Gram Liver = A/B
1	134	16.1	2157.4	85.5	25.2
2	101	25.6	2585.6	99.8	25.9
3	137	17.9	2452.3	83.4	29.4
4	100	15.2	1520.0	23.0	66.1
5	113	10.9	1231.7	34.0	36.2
6	151	12.2	1842.2	36.3	50.7
7	154	25.0	3850.0	76.8	50.1
8	148	12.4	1835.2	46.0	39.9
9	115	21.5	2472.5	69.0	35.8
10	137	20.9	2863.3	58.5	48.9
11	181	24.6	4452.6	54.0	82.5
12	180	27.8	5004.0	64.0	78.2
13	126	21.4	2696.4	68.0	39.7
14	124	21.9	2715.6	53.0	51.2
15	122	22.3	2720.6	46.0	59.1
16	137	24.4	3342.8	66.0	50.6
17	152	16.3	2477.6	41.0	60.4
18	130	24.1	3133.0	24.0	130.5
19	69	25.2	1738.8	42.0	41.4
20	126	14.0	1764.0	41.0	43.0
21				52.5	
22				94.0	
23				46.5	
24				90.0	
25				11.0	
26				64.0	
27				41.0	
28				64.0	
29				30.0	
30				57.5	
31				53.5	
32				55.0	
33				52.0	
34				29.0	
35				39.0	
36				39.0	
37				73.0	
38				70.0	
39				130.0	
40				34.0	
41				31.0	
42				48.0	
43				29.5	
44				19.0	
45				77.0	
46				91.0	
47				37.0	
48				74.0	
49				44.0	
50				50.0	
51				75.0	
52				29.5	
53				69.0	
54				91.0	
55				48.0	
56				36.0	
57				41.0	
58				26.0	
59				26.0	
60				53.0	

Table III. CYP2E1 Content and TCE Metabolic Activity Used to Produce Data Set 3, Describing Parameter D

Samples	Sample Number (from Reference 17)	pmol TCE Oxidized/min/mg MSP (from Reference 17)	pmol CYP2E1/ mg MSP (from Reference 15)[a]	pmol TCE Oxidized/ min/pmol CYP2E1 (Parameter D)
61	HHM 67	1113	11	101.2
62	HHM 84	1724	64	26.9
63	HHM 86	1039	44	23.6
64	HHM 88	1432	50	28.6
65	HHM 55	1422	52.5	27.1
66	HHM 60	1746	91	19.2
67	HHM 77	943	19	49.6
68	HHM 78	1627	77	21.1
69	HHM 81	1416	37	38.3
70	HHM 82	2353	74	31.8
71	HHM 89	890	30	29.7
72	HHM 144	1584	30	53.7
73	HHM 58	2078	94	22.1
74	HHM 61	2623	90	29.1
75	HHM 79	3455	91	38.0
		Geometric Mean		32.5
		Geometric Standard Deviation		1.538

[a]Data not used in estimation of parameter B.

to yield V_{max} values expressed as pmoles TCE oxidized/minute/pmol CYP2E1 (Table III). This measure (parameter D) and its distribution are referred to as data set 3 and are described as TCE_{CYP2}.

2.5. Statistical Analysis

Tables II and III summarize the data employed in the statistical analyses.

Probability distributions were fitted by the SAS© 8.0 Analyst routine to data describing the following variables (with mnemonic variable name): A = pmol CYP2E1/gram liver ($CYP2_{Liv}$); B = pmol CYP2E1/mg MSP ($CYP2_{MSP}$); C = mg MSP/gram liver (MSP_{Liv}) = A/B. StatFit software was used to determine an optimal distribution fit to the 15 observations for parameter D, pmoles TCE oxidized, min/pmol CYP2E1 (TCE_{CYP2}). The log-normal distribution was selected with parameters $\mu = 3.4812$ and $\sigma = 0.4156$ for the imbedded normal distribution, implying a geometric mean and standard deviation of 32.5 and 1.515, and an arithmetic mean and standard deviation of 35.4 and 15.4. This distribution was accepted via chi-squared, Kolmogorov-Smirnov, and Anderson-Darling statistical tests at the $\alpha = 0.05$ (95%) confidence level.

Three sets of data were available: a set of $n = 60$ samples, for which laboratory measurements were available on B = ($CYP2_{MSP}$), an $n = 20$ subset of the 60 samples, for which several additional laboratory measurements were available (PRO_{Liv}, $CYP2_{Pro}$, $CYP2_{MSP}$), and a set of $n = 15$ samples, for which one laboratory measurement was available (TCE_{CYP2}). These three sets of available data were first analyzed separately. The additional variables ($CYP2_{Liv}$ and $C = MSP_{Liv}$) were calculated from the measurement data.

For all variables, normal, log-normal, exponential, and Weibull distributions were fit using standard statistical tests of goodness-of-fit (Kolmogorov-Smirnoff, Cramer-von Mises, and Anderson-Darling) and a visual examination of quantile-quantile plots. The null hypothesis was that the distribution fit the data well, with a rejection of the null at $p \leq 0.10$. All these analyses were performed using SAS©. Each of the distributions was adequately approximated by a log-normal distribution, the parameters of which are the mean (μ) and standard deviation (s) of the logarithms of the observations.

2.5.1. *Analysis via Method of Moments*

For convenience, ignoring the dependence between data set 2 and the $n = 20$ (matched subset) of data set 1, and because the consistency of goodness-of-fit of the data to the log-normal distributions (excluding data set 3: TCE_{CYP2}; pmol TCE oxidized/min/pmol CYP2E1), we applied the

statistical method of moments (addition of errors, (Equation (5)) to combine data sets 1–3 to estimate parameter E, pmol TCE oxidized/min/gram liver. All goodness-of-fit p-values were greater than 0.15. As a convenience, the log-normal parameter will be represented by the geometric mean (GM = e^{μ}) and geometric standard deviation (GSD = e^{s}), respectively, in this article. Equation (5) demonstrates the method used to estimate the distribution of V_{max} values, where the distributions for parameters B (pmol CYP2E1/mg MSP), C (mg MSP/gram liver), and D (pmol TCE oxidized/min/pmol CYP2E1) are combined mathematically. The values at the 5th (X_{05}) and 95th (X_{95}) percentiles for the resulting distribution (parameter E, pmoles TCE oxidized/min/gram liver) were calculated by Equations (6) and (7), respectively.

$$\text{Lnorm}\left[\mu=\mu_1+\mu_2+\mu_3, s=\sqrt{(s_1^2+s_2^2+s_3^2)}\right] \quad (5)$$

where μ_i is mean of logs of observations, s_i is standard deviation of logs of observations, 1 is data set 1—($CYP2_{MSP}$), 2 is data set 2—(MSP_{Liv}), 3 is data set 3—(TCE_{CYP2}).

$$X_{05} = e^{[\mu-1.645\times s]} \quad (6)$$

$$X_{95} = e^{[\mu+1.645\times s]} \quad (7)$$

2.5.2. *Analysis via Computational Statistics*

We next sought to model the distribution of A = pmol CYP2E1/gram liver with greater precision by using all of the available data, including the correlation (Fig. 3) on variables B = pmol CYP2E1/mg MSP and C = mg MSP/gram liver. Since A = B × C, these three variables are not statistically independent. Moreover, it is perhaps not obvious how or whether the 40 measurements of B that are *not* matched to measurements on A and C (observations 21–60 in Table II) can be used to improve estimation of the distribution of A. However, we were able to synthesize and apply two techniques from computational statistics—mixture distribution modeling[28] and classification trees[29,30]—to use all of the B and C data, including the 40 unmatched measurements on B, to model the distribution of A.

The methodology for estimating the frequency distribution of A using all available measurements (i.e., using the joint distribution of A and B, as well as the derived variable C) was as follows.

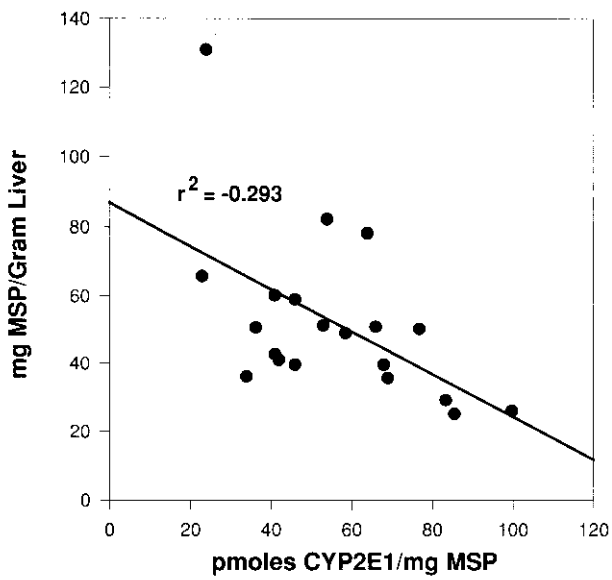

Fig. 3. Correlation between mg MSP/gram and pmol CYP2E1/mg MSP. The slight, but statistically significant, correlation between the two parameters dictated the choice of statistical methods. Data from Reference 27.

1. The frequency distribution for A can be expressed using marginal and conditional probabilities as follows:

$$\begin{aligned}\Pr(A=a) &= \Sigma_{(b,c)}\Pr(A|B=b\ \&\ C=c)\\ &\quad \Pr(B=b\ \&\ C=c)\\ &= \Sigma_{(b,c)}\Pr(A|B=b\ \&\ C=c)\\ &\quad \Pr(B=b)\Pr(C=c|B=b)\end{aligned}$$

   where the sum (or integral) is taken over all (b, c) pairs of values. Thus, A is interpreted as having a distribution that depends on the (perhaps unobserved) values of B and C.
2. The terms Pr(A | B = b & C = c), Pr(B = b), and Pr(C = c | B = b) are estimated empirically from all of the available data using a classification tree estimator. Fig. 4 shows the classification tree fit to the first 20 cases in Table II, i.e., those with data on both A and B (and hence C). This tree provides an estimate of the distribution of A conditioned on the values of B and C. The fit was performed using the KnowledgeSeeker™ package (http://www.angoss.com/ProdServ/indexH.html). Interpretively, the distribution of A is modeled as a finite mixture distribution[28] with a number of components to be estimated from the data. These components correspond to leaves in the classification tree in Fig. 4.

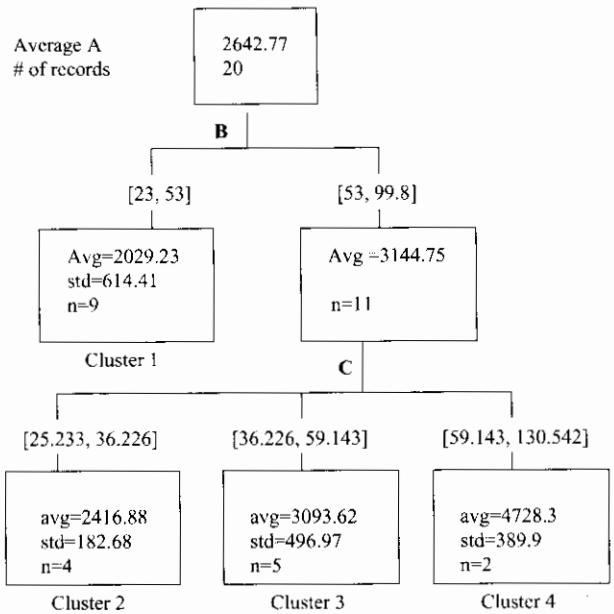

Fig. 4. Classification tree model for the distribution of A = pmol CYP2E1/gram liver. The distribution of A is modeled as a finite mixture distribution with components corresponding to the leaves in the depicted classification tree. The conditional distribution of A depends on which component distribution a case belongs to. The components are bounded by breakpoints in the observed values for B and C. The sample means and sample standard deviations for the four component distributions are estimated from the first 20 cases in Table II.

The conditional distribution of A depends on which component distribution a case belongs to. Fig. 4 shows the sample means and standard deviations for four component distributions (leaves), estimated from the first 20 cases in Table II. Using only these data, the estimated distribution of A would correspond to the following finite (4-component) mixture distribution:

Cluster 1: weight = 9/20, sample mean = 2029.23, sample standard deviation = 614.41

Cluster 2: weight = 4/20, sample mean = 2416.88, sample standard deviation = 182.68

Cluster 3: weight = 5/20, sample mean = 3093.62, sample standard deviation = 496.97

Cluster 4: weight = 2/20, sample mean = 4728.3, sample standard deviation = 389.9

Here, the four components are termed "clusters" since they correspond to sets of cases for which the distribution of A values is approximately the same (i.e., the classification tree algorithm is unable to find any statistically significant difference among them).

3. This initial tree based on the first 20 (full-data) cases in Table II was refined by using the remaining 40 observations of B values in Table II (i.e, cases 21–60) to better estimate the fraction of all cases for which B < 53 (the defining characteristic of Cluster 1). The pooled estimate from all 60 cases is that 32/60 (= 0.53, 95% CI = 0.40 to 0.66) of A values are drawn from Cluster 1. The revised cluster weights using all 60 observations on B are: 0.53 for Cluster 1; 0.17 for Cluster 2; 0.21 for Cluster 3; and 0.09 for Cluster 4. While the cluster-specific sample sizes are very small ($n = 2$ for Cluster 4), this decomposition of the distribution of A into a weighted mixture of component distributions actually *decreases* the variance in estimates of the true mean (and other statistics) of A compared to using a single estimated distribution.[31]

The methodology summarized in Steps 1–3 can be further refined, e.g., by using resampling to establish robust boundaries for the classification tree splits, or by using a Bayesian posterior distribution for the fraction of cases belonging to different clusters. However, given the small number of cases ($n = 20$) with full data, additional refinements of the tree estimator in Fig. 4 with the cluster weights obtained from all 60 measurements for B are not expected to greatly improve the estimation of the distribution of A.

2.6. Combination of Data Sets

A program was developed in the MATLAB software (see Appendix A) to produce A, D, and A × D random variates in accordance with the distributions for A and D derived above. The distribution of A was taken from that determined by computational statistics. This program identified 100,000 random variates. Eight thousand of the generated A × D values were selected at random and were subjected to a further analysis to find an optimal distributional fit (StatFit has a limit of 8,000 values).

2.7. PBPK Model

Human metabolism of TCE was simulated using the PBPK model of Allen and Fisher[32] and

SimuSolv software (Dow Chemical Co., Midland, MI). The model structure consisted of four tissue compartments (liver, rapidly perfused tissues, slowly perfused tissues, and fat) and a gas exchange compartment (lung) connected by blood flows. All TCE biotransformation was assumed to take place in the liver and follow Michaelis-Menten kinetics. The liver was described as a well-stirred homogeneous compartment. Previous studies have demonstrated that more complex heterogeneous models of the liver, such as the parallel tube and dispersion models, were not better than the simple well-stirred model at predicting the *in vivo* clearance of 28 drugs from *in vitro* data.[33] The model was set to simulate two extreme exposure scenarios: (1) simulating a higher, but permitted, occupational exposure at the Threshold Limit Value (TLV) for TCE, which is 50 ppm in air for an 8-hour working day,[34] and (2) simulating a low-dose environmental exposure via drinking water containing the maximally allowable concentration of TCE (5 ug/L).[35] With knowledge that the hepatic metabolism of TCE *in vivo* is limited by blood flow, the model was set to simulate a "worst case" scenario of an oral bolus dose, because this (rather than a slower oral ingestion rate) would be the more likely scenario to produce differences in the amount of TCE metabolized (AML). AML is presented in units of mg TCE metabolized over the course of the simulation per liter of liver tissue. Simulations of AML (amount of TCE metabolized in the liver compartment) were evaluated because the CYP2E1-dependent oxidation of TCE is a required step in the formation of the hepatotoxic metabolite, trichloroacetic acid (TCA), *in vivo*. Chloral hydrate, the oxidative metabolite of TCE, does not have a measurable half-life *in vivo* following its formation from TCE, but is immediately converted to TCA and trichloroethanol. For these simulations, the model incorporated both extremes of the distribution of the V_{max} for TCE oxidation (5th and 95th percentiles).

3. RESULTS

3.1. Distribution of CYP2E1 to Human Hepatic MSP

Analysis of 60 samples of MSP derived from individual adult human organ donors for the content of CYP2E1 (pmoles CYP2E1/mg MSP, parameter B, data set 1) indicated that the log-normal distribution adequately represented the set of observations. The geometric mean and geometric standard deviations required to reconstruct the overall distribution and simulate the value for a percentile of interest are presented in Table IV. These values agree well with those reported by Shimada *et al.*[36] Variance between the values at the 5th and the 95th percentiles of the distribution was approximated fourfold.

3.2. Distribution of CYP2E1 to Intact Human Liver

Three types of analytical procedures were used to determine the distribution of CYP2E1 to intact liver tissue (pmoles CYP2E1/gram liver, parameter A) derived from adult human organ donors. First, the most direct measure, but one for which only 20 observations are available, is depicted in Equations (1) and (2) and involved the application of the ELISA technique to liver homogenate (post 100 × *g*) protein. The empirical distribution of the 20 observations indicates that the magnitude of variance between the observations representing approximately the 5th and 95th

Table IV. Distributions of TCE Metabolism Rate Constant, Microsomal Protein, and CYP2E1 Content of Adult Human Liver

Parameters	A	B	C	D	E
Description	$CYP2^{a}_{Liv}$ (Derived)	$CYP2^{b}_{MSP}$ (Data Set 1)	MSP^{c}_{Liv} (Data Set 2)	TCE^{d}_{CYP2} (Data Set 3)	TCE^{e}_{Liv} (Derived)
Distribution	Discrete	Log Normal	Log Normal	Log Normal	Log Normal
GM	2562	48.9	52.9	32.5	78,810
GSD	930	1.6	1.476	1.515	1.7274
Range	1232–5004	11–130	27–108	19.2–101.2	–
5th Percentile	1232	22.5	27.9	16.4	32,069
95th Percentile	4453	106	100	64.4	193,679

[a]pmoles CYP2E1/gram liver; data are presented as the arithmetic mean, arithmetic standard deviation, and values at the 5.89th and 95.5th percentiles, $n = 20$. GM and GSD derived by computational statistics.
[b]pmoles CYP2E1/mg MSP, $n = 60$.
[c]mg MSP/gram liver, $n = 20$.
[d]V_{max} of CYP2E1 in human liver MSP toward TCE, pmoles/min/pmol CYP2E1, $n = 15$.
[e]V_{max} as pmoles TCE oxidized/min/gram liver, derived via computational statistics.

percentiles of the empirical distribution is approximately threefold. These raw data indicate a mean value of 2,643 and a standard deviation of 962 pmoles CYP2E1/gram liver.

Second, the application of the statistically limited method of moments required the characterization of the two underlying distributions: (1) parameter B, pmoles CYP2E1/mg MSP, data set 1 and (2) parameter C, mg MSP/gram liver, data set 2. Because the observations in these two sets of data were adequately fit by a log-normal distribution, the values for the geometric mean and geometric standard deviations for each data set (Table IV) were combined (Equation (4)). The log-normal distribution of the liver content of MSP (parameter C) was characterized by a geometric mean of 52.9 mg MSP/gram liver and a geometric standard deviation of 1.476 (arithmetic mean and standard deviation of 57 ± 23 mg MSP/gram liver). The MSP content of CYP2E1 (parameter B) was determined in a sample set of 60, and demonstrated a log-normal distribution, with a geometric mean of 48.9 pmoles CYP2E1/mg MSP and a geometric standard deviation of 1.6. The arithmetic mean $\pm$ standard deviation was 54 ± 23 pmoles CYP2E1/mg MSP. When combined, the results indicated a geometric mean of 2,587 pmoles CYP2E1/gram intact adult human liver, with a geometric standard deviation of 1.48. From analysis via Equations (5) and (6), these parameter values indicate values at the 5th and 95th percentile of the distribution to be 949 and 7,053 pmoles CYP2E1/gram. These values are similar to those indicated by the direct measurement of CYP2E1 in homogenate protein, above. These data indicate that the central 90% of the population represented by these 60 adult organ donors expresses a CYP2E1 content that varies 7.4-fold.

Finally, a specific probability distribution for the parameter A was developed, based upon the clusters derived in Section 2.5.2. Recall that clusters of values for A were identified, into which values for parameter B (pmoles CYP2E1/mg MSP) were segregated. In this manner, the influence of parameter B, or its determinant qualities, on parameter A was characterized. A continuous probability distribution was not fit to the individual clusters due to the small number of observations within each cluster; instead, the distribution of A was assumed to be discrete and consist only of the observed values (4th column, Parameter A, of Table II). Clusters were assumed to occur with proportional frequencies equal to the weights {0.53, 0.17, 0.21, 0.09} and to have counts of {9, 4, 5, 2} as described previously. Within a cluster, each value belonging to that cluster is assumed to occur with equal frequency. This approach provides probabilities of 0.53/9 (= 0.0589) for values in Cluster 1, 0.17/4 (= 0.0425) for values in Cluster 2, 0.21/5 (= 0.0420) for values in Cluster 3, and 0.09/2 (= 0.0450) for values in Cluster 4. Cluster statistics are presented in Fig. 4. If we use x_i to represent the ith value of parameter A, and p_i to represent the probability of the ith value, then the mean of the resulting distribution is

$$\sum_{i=1}^{20} p_i x_i = 2561.77 \tag{8}$$

while the variance of the distribution is

$$\sum_{i=1}^{20} p_i x_i^2 - \left(\sum_{i=1}^{20} p_i x_i \right)^2 = 865,563.40 \tag{9}$$

providing a standard deviation of 930.36.

Note that the mean of the raw data for parameter A (Table II) is 2,642.8 while the standard deviation (using Equation (9)) is 937.21 (the sample standard deviation is 962). We see that accounting for the influence of parameter B has shifted our estimates of parameter A slightly downward, and has slightly decreased the standard deviation. This is a result of the individual probabilities being shifted slightly upward or downward from 0.05 in accordance with the distribution shown in empirical distribution. This distribution was used in the recombination of data describing parameter A with data describing parameter D, as discussed below.

3.3. *In vitro* Metabolic Rate Constant (V_{max})

The V_{max} for the oxidation of TCE by CYP2E1 (pmoles TCE oxidized/min/pmol CYP2E1, parameter D, data set 3, Table III) was evaluated in a data set of 15 samples. The apparent V_{max} observed *in vitro* (pmoles TCE oxidized/min/mg MSP) was converted to the more specific units of pmol TCE oxidized/min/pmol CYP2E1 by dividing the observed V_{max} value by the content of CYP2E1 in the MSP (pmoles CYP2E1/mg MSP). The resulting set of 15 observations (pmol TCE oxidized/min/pmol CYP2E1) were fit optimally with the log-normal distribution; its parameters were $\mu = 3.4812$ and $\sigma = 0.4156$ for the embedded normal distribution, implying a geometric mean and standard deviation of 32.5 and 1.515, and an arithmetic mean and standard deviation of 35.4 and 15.4. This distribution was accepted via chi-squared, Kolmogorov-Smirnov, and Anderson-Darling statistical tests at the $\alpha = 0.05$

(95%) confidence level. The difference between values at the 5th and 95th percentiles of the distribution approximated fourfold.

3.4. Determining the Metabolic Capacity of Intact Tissue and Extrapolation of Units

MATLAB results of the simulations of 100,000 random variates of A × D revealed a plot (not shown) suggestive of a log-normal distribution, and a normal distribution (not shown) of the logs of values of A × D. StatFit analyzed 8,000 of these variates, and indicated that the most likely distribution was the log-normal, with parameters $\mu = 11.2748$ and $\sigma = 0.5466$. The log-normal distribution was accepted via chi-squared, Kolmogorov-Smirnov, and Anderson-Darling statistical tests at the $\alpha = 0.05$ (95%) confidence level. The parameters of the log-normal distribution indicate a geometric mean of 78,810 pmoles TCE oxidized/minute/gram liver, and a geometric standard deviation of 1.7274. Applying these values in Equations (6) and (7) results in 5th and 95th percentile values of 32,069 and 193,679 pmoles TCE oxidized/minute/gram liver, respectively. These values were corrected for molecular weight, time, and fractional composition of the body represented by the liver (liver weight = 2.6% body mass) to yield values of 23.514 and 142.01 mg/h/kg at the 5th and 95th percentiles of the distribution, respectively.

3.5. PBPK Model Predictions

The PBPK model for TCE was used to simulate exposure of a 70 kg male human to 50 ppm TCE for 8 hours. This exposure scenario represents the maximum recommended exposure of an individual to TCE in the workplace. The extremes of expression of the CYP2E1-mediated oxidation of TCE in the liver used here (approximately six-fold) resulted in a difference in TCE hepatic metabolism of approximately 2% (Table V). For this simulation, the amount of TCE oxidized over the exposure period per volume of liver (μg/L) was used as the dose metric most linked with hepatotoxic injury/risk. Simulation of the oral ingestion of TCE (5 μg/L) in 2 L of drinking water using the 5th and 95th percentiles of the TCE oxidation rate gave similar results (Table V). These data indicate that physiological processes limit the full impact of the differences in CYP2E1 activity toward TCE mediating the formation of toxic metabolites. Previous PK analyses of the effect of enzyme induction on the bioactivation of TCE and other volatile organic compounds indicated a hepatic blood flow limitation of the bioactivation process.[14] The rate of blood flow delivery of these substances to the liver is much slower than the rate of bioactivation in the liver, limiting the impact of enzyme induction or interindividual variability. This study focused on the issue of whether enzymic variance alone could contribute substantially to susceptibility to hepatotoxic injury, and did not attempt to capture or examine the effect of other factors (e.g., differences in hepatic blood flow) on the PK of TCE.

Table V. Effect of Human Hepatic CYP2E1 Activity Distribution on the Bioactivation of TCE Following an Inhalation and an Oral Exposure

	Liver Metabolites (ug/L)	
Oxidation Rate	Inhalation[a]	Oral[b]
5th percentile (23.514 mg/h/kg)	258.3	5.4
95th percentile (142.01 mg/h/kg)	264.9	5.5
Difference (%)	2	2

[a] Simulations of 8-hour exposure to TCE (50 ppm) by a 70 kg male human as described under Methods.
[b] Simulations of exposure to TCE in drinking water (5 μg/L; 2 L) over 24 hours by a 70 kg male human as described under Methods.

4. DISCUSSION

Advanced PK studies and PBPK modeling allow the development of the linkage between external dose and target tissue dosimetry. PBPK models can predict target tissue concentrations associated with specific levels of response in animals or humans (LOAEL, NOAEL, or BMD-derived level of response). Human PBPK models can examine the risk-relevant PK outcome of chemical exposure (i.e., tissue levels of bioactive metabolite) and predict the external exposure (i.e., mg/kg/day) required to produce this PK outcome at the same level observed in research animals at the corresponding level of toxicity. When adequate information is available to quantify the metabolism to or from the bioactive chemical form, the human PBPK model can be further refined to include data on enzyme (metabolic) variance in human tissues. Then the PBPK models can be exercised to examine not only animal to human differences in the risk-relevant PK outcome, but also the human interindividual variance in the expression of that PK outcome.

Biotransformation is a critical determinant of both PK and risk since metabolism is involved in the bioactivation and detoxication of xenobiotics.

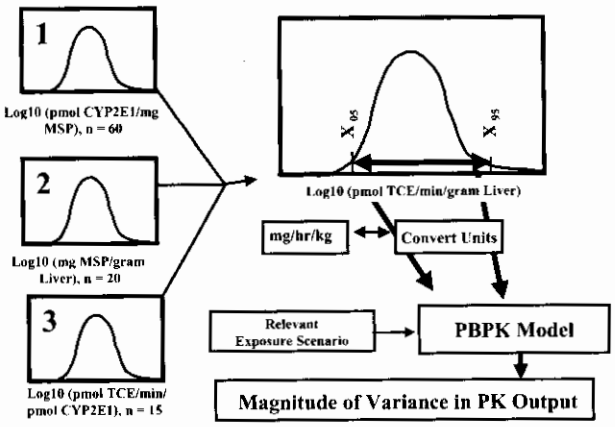

Fig. 5. Extrapolation and incorporation of *in vitro* derived metabolic rates in PBPK modeling. This figure depicts the framework for deriving appropriate *in vitro* measures and their extrapolation into a PBPK model. The model was exercised to simulate environmentally and occupationally relevant exposures.

Genetic polymorphisms and enzyme induction due to environmental and lifestyle factors can affect the level of expression of xenobiotic metabolizing enzymes. Thus, genetic polymorphisms become critical to risk only when they alter PK outcomes. The refinement of human health risk assessments for chemicals metabolized by the liver to reflect data on human interindividual PK variability can be accomplished through (1) the characterization of enzyme expression in large banks of human liver samples, (2) the employment of appropriate techniques for the quantification and extrapolation of metabolic rates derived *in vitro*, and (3) the judicious application of PBPK modeling.

Numerous PK outcomes may be simulated by PBPK modeling; the identification of the risk-relevant PK outcome(s) from toxicity studies allows the study of their variability through adequately constructed PBPK models. When PK models are constructed to include metabolic rates (and rate constants) derived *in vitro*, several extrapolations are necessary, not the least of which is the extrapolation of enzyme content (Fig. 5). PBPK models include the apparent V_{max} expressed as mg/h/kg body mass, while typical *in vitro* studies express V_{max} in terms of nmoles product formed/minute/mg microsomal protein. Accurate extrapolation requires initially that enzyme content be expressed per unit intact liver (i.e., pmoles CYP2E1/gram liver), and the extrapolation has usually included a numerical estimation of the MSP content of liver (i.e., 50 mg MSP/gram liver). The MSP content of intact liver has been measured and used to extrapolate *in vitro*-derived metabolism kinetic constants for use in PBPK modeling efforts in humans[37,38] and to infer measures of intrinsic clearance (Clint) in traditional rat-based PK models.[39] In the previous PBPK-based approach for TCE,[37] samples expressing extreme values for kinetic constants (K_M and V_{max}) were chosen for extrapolation to a PBPK model. Those extrapolations were based on the hepatocellularity of intact liver tissue, and on microsomal protein content of liver, rather than the content of CYP2E1 of liver. The V_{max} value was not previously extrapolated on the basis of CYP2E1 content as no data existed at the time through which to quantify the distribution of the key metabolic enzyme within human liver. With respect to the distribution of the cytochromes P450 in one preparation of human liver (microsomes), several investigations[17,36,40,41] have revealed quantitative information about the content of these multiple enzyme forms in this preparation, but reveal no direct information on the type of distribution (i.e., log-normal) of the enzymes within MSP, their content or distribution to the intact liver *in situ*. In the present study, we developed measures of the liver content of microsomal protein, of which the CYP enzymes (and other important xenobiotic-metabolizing enzymes, i.e., glucuronyl transferases) are a constituent. This key piece of information is necessary to estimate the content of the enzyme(s) in the intact liver. By combining the two data sets on (1) the MSP content of CYP (pmoles CYP/mg MSP), and (2) the liver content of MSP (mg MSP/gram liver), we derived the liver content of CYP (pmoles CYP/gram liver), and developed measures of that variance, employing a total number of 60 samples derived from adult human organ donors. The approach also included the determination and inclusion of the human interindividual variance in metabolic activity toward TCE derived in an additional set of 15 samples. This analysis allowed the variance of that critical enzyme kinetic parameter (V_{max}) to be examined among humans, and expressed as pmoles TCE oxidized per minute per pmol CYP2E1. This parameter (pmol TCE oxidized/min/pmol CYP2E1) did vary among the human samples evaluated, not surprisingly. This may be explained, in part, by potential underlying genetic differences impacting CYP2E1 activity, differences in the presence of other CYP forms that also metabolize TCE at higher concentrations, and human-to-human interindividual differences in the lipid composition (both qualitative and quantitative) of isolated MSP preparations. The activity of isolated enzymes represents the functional status of their respective donors. The stability of these enzymes upon

isolation and storage seems not to be a major contributor to this variance. The level of detail in this expression of V_{max} allowed for a direct combination with information on the variance of CYP2E1 in intact human liver, which enabled the resulting PBPK analysis of the impact of that variance on the risk-relevant pharmacokinetic (PK) outcome, amount of TCE metabolized in the liver, among adult humans. Together, these data sets separately describing enzyme activity and enzyme content combine to describe the metabolic capacity of the liver. The resulting combined distribution for the V_{max} value demonstrated that this parameter (mg/h/kg) differed more than six-fold between the values at the 5th and 95th percentiles of the distribution. When these values were separately integrated into the PBPK model, resulting estimates of the amount of TCE oxidized over the exposure period differed by only 2%. Thus, widely divergent values for apparent V_{max}, resulting from both variance in enzyme content and activity, had little effect on the *in vivo* metabolism of TCE, and will have little effect on the hepatotoxic injury following TCE exposure in humans.

The present work demonstrates a significant advantage over earlier studies in that statistically valid and robust measures of enzyme content and enzyme activity have been developed and incorporated into the PBPK-based approach. This advance allows the application of the approach to estimate population distributions of risk, when chemical dose-response parameters (e.g., slope factors) are available. With the availability of large banks of well-characterized subcellular fractions (mainly hepatic MSP) derived from the livers of human organ donors comes the opportunity to determine several measures of human biochemical individuality, which will be applicable to many environmental, occupational, and therapeutic compounds. Although several investigations have failed to identify an inverse relationship between post mortem cold-clamp time (the time interval between the perfusion, removal, and refrigeration of liver tissue and the freezing of the tissue or microsomal protein isolation) and microsomal enzyme activity, the assumption that the activity of these enzymes *in vitro* represents their activity *in vivo* must be recognized as such. From these samples, we can measure interindividual differences in enzyme activity and differences in enzyme content in isolated MSP. The *in vitro* metabolism of several CYP2E1 substrates, such as furan,[41,43] perchloroethylene,[37] and trichloroethylene,[38] have been successfully extrapolated to the *in vivo* setting through application of adequately developed and validated PBPK models. The additional validation of the extrapolation procedure for metabolic activity based on enzyme recovery data is important. This demonstrates the applicability of the methodology to determine the interindividual differences of risk-relevant PK outcomes (i.e., the amount of metabolite formed in the liver for a bioactivated hepatotoxicant) for xenobiotics to which humans cannot be safely exposed for the generation of experimental data. It is anticipated that toxicological data can be generated in test species *in vivo* and *in vitro* to determine the metabolic species responsible for toxicity, the PK of the xenobiotic and metabolite(s), and the identity of the enzyme responsible for metabolism. With this information, an adequate test animal-based PBPK model can be extrapolated to humans, using human tissue partition coefficients and the appropriate physiological parameters. Data on human enzyme recovery could be used to develop appropriate bounds on the distribution of metabolic activity for evaluation with the PBPK model to represent predefined proportions of the population.

The successful application of this approach requires the avoidance of several pitfalls. It requires (1) the metabolic process under investigation must be as directly linked to the risk-relevant PK outcome as possible: the correct identification of the critical toxic effect, against which protection is warranted, or toward which susceptibility requires evaluation. In the absence of a defined link between this effect and its most closely related and measurable or predictable PK outcome (e.g., AML), then further effort will not advance the goals of the approach. (2) The tissues/preparations included in the experiments must be viable. The reliance on human tissues of research grade can be troublesome; the comparison of *in vitro*-derived metabolic rates and rate constants, especially in humans, requires some justification that these *ex vivo* or *in vitro* systems maintain the metabolic capacity they possess *in vivo*. The isolated hepatocyte model is more closely related to the *in vivo* situation than the isolated microsomal protein preparation, but metabolic rates from both systems require extrapolation based on recovery information to the *in vivo* situation. Reliance upon data derived from compromised *in vitro* systems can lead to underpredictions of *in vivo* metabolism. The inclusion of data from compromised systems (i.e., lengthy 37° incubations of microsomal protein, the application of immortalized cell lines, etc.) must be avoided. The evaluation of metabolic activity toward recognized marker substrates and

assessment of cellular viability provide some evidence of *in vitro* system stability. (3) There must be sufficient data to enable extrapolation based on protein recovery. Lack of data or uncertainty in the available data quantifying the relationship between the *in vitro* system and the *in vivo* situation greatly complicate the extrapolation procedure. Values for hepatocellularity in rats and humans, and values for microsomal protein content of rats and humans, are available for use in extrapolation procedures. (4) The derivation of metabolic rate constants must be accomplished under valid experimental conditions. Rate constants must be derived under conditions where rate is proportionate to an increase in protein content, over time and with increasing substrate concentrations (for first-order reactions). The value of such data is enhanced when rate constants are tied specifically to the enzyme, rather than the subcellular fraction (e.g., pmoles/min/pmol CYP2E1 vs. pmoles/min/mg MSP). (5) Data should be used to identify the pertinent enzyme; the contribution of more than one enzyme complicates enzyme kinetic evaluations. Additional uncertainty is encountered in the metabolic evaluation of substrates, toward which multiple enzymes are active. Given the human interindividual variability on enzyme expression as a result of genetic, dietary, and lifestyle choices, different ratios of two potentially active enzymes may be observed. In this instance, the approach to *in vitro* enzyme kinetic investigations must be robust enough to separately identify the kinetic constants applicable to each of the enzymes. Kinetic constants derived for the preparation, without regard to the pertinent enzymes, can falsely indicate that the apparent V_{max} value is shifted upward due to the contribution of a low affinity form, when *in vivo* substrate concentrations would not be sufficient to drive an appreciable contribution of this enzyme to the reaction. (6) This approach relies on the availability of a "validated" PBPK model. While generalization of model structure and physiological components across chemicals is often the case, the models must include parameters demonstrated or judged to be relevant to the study chemical. In addition to metabolic rate constants, tissue partition coefficients (PC) are highly chemical-specific, and differ for the same tissue type among species. The application of PC values derived in other species or adapted from PC values of related chemicals requires justification. (7) Finally, the approach is aimed specifically at quantifying human interindividual differences in metabolic capacity. This approach is not specifically aimed at quantifying human interindividual PK difference for TCE oxidation; it was developed to test the hypothesis that variability in metabolic capacity alters susceptibility to hepatotoxic injury from TCE exposure. The approach here demonstrates the applicability of the statistical bounds established for the population under investigation. In that regard, the application of a representative sample set is required. The data must support the identification of distribution type and include enough observations so that confidence can be placed in the identification of values at predetermined points of the distribution. While these are some of the general pitfalls, investigators trained in the disciplines of the individual investigatory steps will be quite familiar with many of the more technical pitfalls.

To members of the risk assessment community who are advocating the development of approaches that provide more information than just "safe exposure limits" (e.g., RfC and RfD values), the present approach may be useful. The approach is centered on the identification of the risk-relevant PK outcome through evaluation of toxicity and PK investigations, not necessarily through PBPK investigations. Under optimal conditions, the linking of PBPK modeling approaches with data describing human biochemical individuality (enzyme content and enzyme activity) will allow the quantification of the PK component of UFH. The collection of advanced measures of human biochemical individuality (e.g., differences in the liver's content of critical xenobiotic metabolizing enzymes) will broaden the applicability of this approach to other chemicals whose PK are modulated by the same enzyme. It is conceivable that when this parameter (enzyme content and activity) modulates the production of the risk-relevant PK outcome, information about the population distribution of the parameter (i.e., hepatic content of CYP2E1) will lead to applications demonstrating the fraction of the population that will be protected by regulations that specify a given level of chemical exposure. Similarly, with carcinogenicity slope factors, risk-relevant PK outcomes can be converted directly to measures of risk, indicating the level of risk corresponding to a given level of enzyme content and activity. By converting exposure to tissue dose, and having information to link tissue dose to risk, the PBPK modeling approach may be usefully employed to develop distributions of risk, rather than simply assessing or demonstrating the health protective nature of a given exposure.

The purpose of the present study was to explore the potential advantage of including additional, specific information on human biochemical individuality as a process to refine the human health risk assessment process. Because an ever-increasing amount of data is

being developed through the analysis of tissues derived not only from surgical resections, but also from human organ donors, these sources of tissues offer a unique potential to increase our knowledge about human biochemical individuality.

5. SUMMARY AND CONCLUSIONS

Human interindividual PK variability is important both for chemicals with adequate human PK data and for those chemicals to which humans cannot be experimentally exposed. Because CYP2E1 activity limits (*in vitro*) the production of oxidative, hepatotoxic metabolites of TCE, we evaluated the distribution of that enzyme in liver from up to 75 adult human organ donors by applying published and accepted biochemical and statistical methods. The extrapolation of *in vitro* data captured both the variance in enzyme content and enzyme activity among adult humans.

CYP2E1 content and metabolic activity toward TCE are described by log-normal distributions. The central 90% of the human population represented by these adult organ donors differs by less than fourfold in the hepatic content of this critical xenobiotic metabolizing enzyme; that same fraction of the population differed by approximately sixfold with respect to the oxidation of TCE. The finding and additional information to be gained from the now-characterized distribution of CYP2E1 to intact human liver will be useful not only to the assessment of risk from TCE exposure, but also to the assessment of risks from other environmental chemicals that are also metabolized by this enzyme, including chloroform, carbon tetrachloride, benzene, toluene, and styrene. Because the metabolism of TCE is limited by blood flow to the liver, divergent values of V_{max} do not result in appreciable differences in the risk-relevant PK outcome, the amount of TCE metabolized in the liver. Therefore, factors that increase the hepatic expression of CYP2E1 and/or its metabolic activity will not always result in proportionate changes in key PK outcomes. This is because of the relatively low solubility of TCE in blood, and the relatively high capacity of the liver to metabolize TCE (due to a relatively high level of expression of the enzyme and the relatively high metabolic activity of the enzyme toward TCE), the limiting factor, *in vivo*, for TCE oxidation becomes the rate at which TCE is delivered to liver tissue by hepatic blood flow. In this situation, increases in TCE metabolic capacity, even from the 5th to the 95th percentiles of the distribution, result in only a 2% increase in the amount of TCE metabolized. With respect to the hepatotoxicity of TCE resulting from exposure scenarios similar to those employed in this analysis, these data indicate that the amount of PK variability attributed to enzymic variance among humans is approximately 2%. The approach described here is especially applicable to chemicals to which humans cannot be experimentally exposed for ethical reasons. The application of actual, not hypothesized, bounds of variance and the definition of the distribution of enzyme content and activity among humans can allow the calculation of finite levels of risk (when dependent on the PK outcome) at different chosen percentiles of the distribution of enzyme content and activity.

Several conditions must first be met for this strategy to be successful:

1. The target organ, mode, or mechanism of action, and metabolic species responsible for toxicity must be known.
2. The target tissue-toxic chemical species dose-response relationship must be known.
3. The biotransforming enzyme must be known and information on the variance and type of its distribution among humans must be known.
4. The kinetic mechanism of metabolism must be known and expressed per unit of enzyme.
5. An adequately characterized PBPK model must be available for adaptation.

We have quantified the extent of variance in enzyme content of a critical xenobiotic metabolizing enzyme, CYP2E1, and the variance in the hepatic biotransformation of a key environmental contaminant, trichloroethylene. The parameters of the resulting log-normal distributions can be used to identify the bounds of biochemical and pharmacokinetic variance (e.g., 90% of the population), within which susceptibility can be determined and allows the replacement of hypothesized magnitudes of difference with actual measurement of such when determining the impact of enzyme variance on risk.

This article identifies the conditions and types of data required, communicates and applies a logical approach, and describes the limitations of the approach in estimating the human interindividual variance of risk-relevant PK outcomes that may signify susceptibility to chemical injury. While data set 3 is unique to TCE, data set 2 will be useful in estimating the hepatic content of all enzymes contained in the microsomal fraction, when their distribution characteristics are known, and the information derived from the combination of data sets 1 and 2 are directly

applicable to other environmental contaminants that are also substrates for CYP2E1.

ACKNOWLEDGMENTS

The views expressed in this article (NCEA-C-0956) are those of the individual authors and do not necessarily reflect the views and policies of the U.S. Environmental Protection Agency (EPA). This research was supported by an interagency agreement between U.S. EPA/NCEA and CDC/NIOSH (No. DW75851501; John C. Lipscomb, Project Officer) and through a cooperative agreement between U.S. EPA/NCEA and Dr. Gregory Kedderis (No. CR828047-01-0; John C. Lipscomb, Project Officer). The authors wish to express their gratitude to Glenn Suter and Bob Bruce (EPA, NCEA, Cincinnati), and Ulrike Bernauer (BgVV, Berlin, Germany) for insightful comments during preparation of the article. Preliminary results from this investigation have been presented at the annual meeting of the Society for Risk Analysis, December 2000, Arlington, VA and December 2001, Seattle, WA; at the annual meeting of the Society of Toxicology, March 2001, San Francisco, CA, and March 2002, Nashville, TN; and at the Spring Toxicology Conference, April 2001, Wright–Patterson Air Force Base, OH. We are sincerely grateful to organ donors and their families; these and other studies would not be possible without their generous contributions.

APPENDIX A: MATLAB CODE TO GENERATE A × D

```
numReps = 250000;
cluster{1} = [1520 1231.7 1842.2 1835.2
  2720.6 2477.6 3133 1738.8 1764];
cluster{2} = [2157.4 2585.6 2452.3 2472.2];
cluster{3} = [3850 2863.3 2696.4 2715.6
  3342.8];
cluster{4} = [4452.6 5004];
clusterCDF = [.53 .70 .91 1.0];
A = zeros(1,numReps);
result = zeros(1,numReps);
for i = 1:numReps
  D = exp(3.4812 +.4156*randn);
  clusterNum = min(find(rand <
    clusterCDF));
  clusterSize = length(cluster{clusterNum});
  clusterIndex = ceil(rand * clusterSize);
  A(i) = cluster{clusterNum}(clusterIndex);
  result(i) = A(i) * D;
end
writeArray = result';
save Dvalues.txt writeArray -ASCII
disp('A parameters')
disp([mean(A) std(A)])
disp('AxD parameters')
disp([mean(result) std(result)])
hist(result,100)
title('Empirical Distribution of A x D')
figure(2)
hist(log(result),100)
title('Empirical Distribution of ln(A x
  D)')
```

REFERENCES

1. Bogdanffy, M. S., & Jarabek, A. M. (1995). Understanding mechanisms of inhaled toxicants: Implications for replacing default factors with chemical-specific data. *Toxicology Letters, 82/83*, 919–932.
2. Jarabek, A. M. (1995). Interspecies extrapolation based on mechanistic determinants of chemical disposition. *Human and Ecological Risk Assessment, 1*, 641–662.
3. Bogdanffy, M. S., Sarangapani, R., Plowchalk, D. R., Jarabek, A. M., & Andersen, M. E. (1999). A biologically-based risk assessment for vinyl acetate-induced cancer and noncancer inhalation toxicity. *Toxicological Sciences, 51*, 19–35.
4. WHO (World Health Organization). (1998). *Guidelines for Drinking Water Quality*. Addendum to Volume 2, *Health Criteria and Other Supporting Information*, 2nd ed. (pp. 15–30). Geneva, Switzerland, ISBN 92-4-1545143.
5. IPCS (International Programme on Chemical Safety). (1994). Environmental Health Criteria 170. *Assessing Human Health Risks of Chemicals: Derivation of Guidance Values for Health-Based Exposure Limits*. Geneva, World Health Organization.
6. IPCS (International Programme on Chemical Safety). (1998). Environmental Health Criteria 204: Boron. International Programme on Chemical Safety, Geneva, Switzerland, World Health Organization, ISBN 92-4157204 3.
7. U.S. EPA. (1999). *Toxicological Review of Ethylene Glycol Monobutyl Ether (111-76-2) in Support of Summary Information on the Integrated Risk Information System (IRIS)*. Available at http://www.epa.gov/iris.
8. U.S. EPA. (2000). *Toxicological Review of 1,3-Dichloropropene (542-75-6) in Support of Summary Information on the Integrated Risk Information System (IRIS)*. National Center for Environmental Assessment, Washington, DC. Available at http://www.epa.gov/iris.
9. U.S. EPA. (2001). *Toxicological Review of Hexachlorocyclopentadiene (77-47-4) in Support of Summary Information on the Integrated Risk Information System (IRIS)*. Available at http://www.epa.gov/iris.
10. U.S. EPA. (1998). *Toxicological Review of Methyl Methacrylate (80-62-6) in Support of Summary Information on the Integrated Risk Information System (IRIS)*. Available at http://www.epa.gov/iris.
11. Lipscomb, J. C., & Kedderis, G. L. (2002). Incorporating human interindividual biotransformation. Variance in health risk assessment. *Science of the Total Environment, 288*, 13–21.
12. Lehninger, A. L. (1975). *Biochemistry*, 2nd ed. (pp. 183–216). New York: Worth.
13. Segel, I. H. (1975). *Enzyme Kinetics* (pp. 1–17). New York: Wiley.
14. Kedderis, G. L. (1997). Extrapolation of *in vitro* enzyme induction data to humans *in vivo*. *Chemico-Biological Interactions, 107*, 109–121.

15. Snawder, J. E., & Lipscomb, J. C. (2000). Interindividual variance of cytochrome P450 forms in human hepatic microsomes: Correlation of individual forms with xenobiotic metabolism and implications in risk assessment. *Regulatory Toxicology and Pharmacology, 32*, 200–209.
16. Arias, I. M., Popper, H., Schachter, D., & Shafritz, D. A. (1982). *The Liver: Biology and Pathobiology*. New York: Raven Press.
17. Lipscomb, J. C., Garrett, C. M., & Snawder, J. E. (1997). Cytochrome P450-dependent metabolism of trichloroethylene: Interindividual differences in humans. *Toxicology and Applied Pharmacology, 142*, 311–318.
18. Northrop, D. B. (1983). Fitting enzyme-kinetic data to V/K. *Analytical Biochemistry, 132*, 457–461.
19. Gut, J., Catin, T., Dayer, P., Kronbach, T., Zanger, U., & Meyer, U. A. (1986). Debrisoquine/sparteine-type polymorphism of drug oxidation: Purification and characterization of two functionally different human liver cytochrome P-450 isozymes involved in impaired hydroxylation of the prototype substrate bufuralol. *Journal of Biological Chemistry, 261*, 11734–11743.
20. Fisher, J. W. (2000). Physiologically based pharmacokinetic models for trichloroethylene and its oxidative metabolites. *Environmental Health Perspectives, 108*, 265–273.
21. Bloemen, L. J., Monster, A. C., Kezic, S., Commandeur, J. N., Veulemans, H., Vermeulen, N. P., & Wilmer, J. W. (2001). Study on the cytochrome P-450- and glutathione-dependent biotransformation of trichloroethylene in humans. *International Archives of Occupational and Environmental Health, 74*, 102–108.
22. Nakajima, T., Okino, T., Okuyama, S., Kaneko, T., Yonekura, I., & Sato, A. (1988). Ethanol-induced enhancement of trichloroethylene metabolism and hepatotoxicity: Difference from the effect of phenobarbital. *Toxicology and Applied Pharmacology, 94*, 227–237.
23. Barton, H. A., & Clewell, H. J. III. (2000). Evaluating the noncancer effects of trichloroethylene: Dosimetry, mode of action, and risk assessment. *Environmental Health Perspectives, 108*, 323–334.
24. Bull, R. J. (2000). Mode of action of liver tumor induction by trichloroethylene and its metabolites, trichloroacetate and dichloroacetate. *Environmental Health Perspectives, 108*, 241–259.
25. Ikeda, M., Miyake, Y., Ogata, M., & Ohmori, S. (1980). Metabolism of trichloroethylene. *Biochemical Pharmacology, 29*, 2983–2992.
26. Guengerich, F. P. (1989). Analysis and characterization of enzymes. In A.W. Hayes, (Ed.), *Principles and Methods of Toxicology* (pp. 777–814). New York: Raven Press.
27. Lipscomb, J. C., Teuschler, L. K., Swartout, J. C., Striley, C. A. F., & Snawder, J. E. (2003). Variance of microsomal protein and cytochrome P450 2E1 and 3A forms in adult human liver. *Toxicology Mechanisms and Methods, 13*, 45–51.
28. Titterington, D. M., Smith, A. F. M., & Makov, U. E. (1985). *Statistical Analysis of Finite Mixture Distributions*. New York: Wiley.
29. Zhang, H., & Singer, B. (1999). *Recursive Partitioning in the Health Sciences*. New York: Springer.
30. Breiman, L., Friedman, J., Olshen, R., & Stone, C. (1984). *Classification and Regression Trees*. Wadsworth, CA: Wadsworth Publishing.
31. Feller, W. (1968). *An Introduction to Probability Theory and Its Applications* Volume 1, 3rd ed., (pp. 229–232). New York: Wiley.
32. Allen, B. C., & Fisher, J. W. (1993). Pharmacokinetic modeling of trichloroethylene and trichloroacetic acid in humans. *Risk Analysis, 13*, 71–86.
33. Houston, J. B., & Carlile, D. J. (1997). Prediction of hepatic clearance from microsomes, hepatocytes, and liver slices. *Drug Metabolism Reviews, 29*, 891–922.
34. American Conference of Governmental Industrial Hygienists (ACGIH). (2001). *Threshold Limit Values for Chemical Substances and Physical Agents and Biological Exposure Indices*. Cincinnati, OH: ACGIH.
35. U.S. EPA. (1987). National primary drinking water regulations; synthetic organic chemicals; monitoring for unregulated contaminants. *Federal Register, 52*(130), 25690.
36. Shimada, T., Tsumura, F., & Yamazaki, H. (1999). Prediction of human liver microsomal oxidations of 7-ethoyxcoumarin and chlorzoxazone with kinetic parameters of recombinant cytochrome P-450 enzymes. *Drug Metabolism and Disposition, 27*, 1274–1280.
37. Reitz, R. H., Gargas, M. L., Mendrala, A. L., & Schumann, A. M. (1996). *In vivo* and *in vitro* studies of perchloroethylene metabolism for physiologically based pharmacokinetic modeling in rats, mice and humans. *Toxicology and Applied Pharmacology, 136*, 289–306.
38. Lipscomb, J. C., Fisher, J. W., Confer, P. D., & Byczkowski, J. Z. (1998). *In vitro* to *in vivo* extrapolation for trichloroethylene metabolism in humans. *Toxicology and Applied Pharmacology, 152*, 376–387.
39. Carlile, D. J., Zomorodi, K., & Houston, J. B. (1997). Scaling factors to relate drug metabolic clearance in hepatic microsomes, isolated hepatocytes, and the intact liver: Studies with induced livers Involving diazepam. *Drug Metabolism and Disposition, 25*, 903–911.
40. Iyer, K. R., & Sinz, M.W. (1999). Characterization of phase I and phase II hepatic drug metabolism activities in a panel of human liver preparations. *Chemico-Biological Interactions, 118*, 151–169.
41. Shimada, T., Yamazaki, H., Mimura, M., Inui, Y., & Guengerich, F. P. (1994). Interindividual variations in human liver cytochrome P450 enzymes involved in the oxidation of drugs, carcinogens and toxic chemicals: Studies with liver microsomes of 30 Japanese and 30 Caucasians. *Journal of Pharmacology and Experimental Therapeutics, 270*, 414–423.
42. Kedderis, G. L., Carfagna, M. A., Held, S. D., Batra, R., Murphy, J. E., & Gargas, M. L. (1993). Kinetic analysis of furan biotransformation by F-344 rats *in vivo* and *in vitro*. *Toxicology and Applied Pharmacology, 123*, 274–282.
43. Kedderis, G. L., & Held, S. D. (1996). Prediction of furan pharmacokinetics from hepatocyte studies: Comparison of bioactivation and hepatic dosimetry in rats, mice, and humans. *Toxicology and Applied Pharmacology, 140*, 124–130.